

Received:  
13 August 2021

Revised:  
21 October 2021

Accepted:  
08 November 2021

© 2022 The Authors. Published by the British Institute of Radiology under the terms of the Creative Commons Attribution-NonCommercial 4.0 Unported License <http://creativecommons.org/licenses/by-nc/4.0/>, which permits unrestricted non-commercial reuse, provided the original author and source are credited.

Cite this article as:

Derks SHAE, van der Veldt AAM, Smits M. Brain metastases: the role of clinical imaging. *Br J Radiol* 2022; **95**: 20210944.

## REVIEW ARTICLE

# Brain metastases: the role of clinical imaging

<sup>1,2,3</sup>SOPHIE H. A. E. DERKS, MD, <sup>2,3</sup>ASTRID A. M. VAN DER VELDT, MD, PhD and <sup>2</sup>MARION SMITS, MD, PhD

<sup>1</sup>Department of Neuro-Oncology, Erasmus MC Cancer Institute, Rotterdam, The Netherlands

<sup>2</sup>Department of Radiology & Nuclear Medicine, Erasmus Medical Center, Rotterdam, The Netherlands

<sup>3</sup>Department of Medical Oncology, Erasmus MC Cancer Institute, Rotterdam, The Netherlands

Address correspondence to: Professor Marion Smits  
E-mail: [marion.smits@erasmusmc.nl](mailto:marion.smits@erasmusmc.nl)

### ABSTRACT

Imaging of brain metastases (BMs) has advanced greatly over the past decade. In this review, we discuss the main challenges that BMs pose in clinical practice and describe the role of imaging.

Firstly, we describe the increased incidence of BMs of different primary tumours and the rationale for screening. A challenge lies in selecting the right patients for screening: not all cancer patients develop BMs in their disease course. Secondly, we discuss the imaging techniques to detect BMs. A three-dimensional (3D) T1W MRI sequence is the golden standard for BM detection, but additional anatomical (susceptibility weighted imaging, diffusion weighted imaging), functional (perfusion MRI) and metabolic (MR spectroscopy, positron emission tomography) information can help to differentiate BMs from other intracranial aetiologies.

Thirdly, we describe the role of imaging before, during and after treatment of BMs. For surgical resection, imaging is used to select surgical patients, but also to assist intraoperatively (neuronavigation, fluorescence-guided surgery, ultrasound). For treatment planning of stereotactic radiosurgery, MRI is combined with CT. For surveillance after both local and systemic therapies, conventional MRI is used. However, advanced imaging is increasingly performed to distinguish true tumour progression from pseudoprogression.

Finally, future perspectives are discussed, including radiomics, new biomarkers, new endogenous contrast agents and theranostics.

### INTRODUCTION

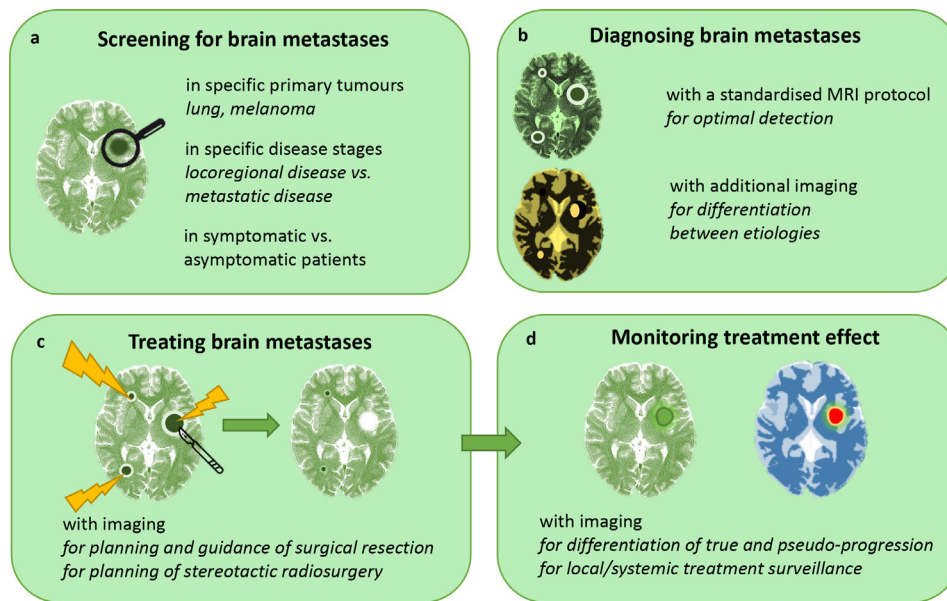
The field of clinical oncology is rapidly changing. With improving treatments, advanced cancer is better controlled, leading to improved overall survival (OS) and even curative.<sup>1</sup> However, brain metastases (BMs) now more often emerge in cancer patients, and they seem to behave differently from extracranial disease. Brain metastases are still associated with poor OS, with an estimated OS rate for all tumour types of 8.1% at 2 and 2.5% at 5 years after diagnosis.<sup>2</sup>

In BMs, the efficacy of most systemic anticancer therapies is reduced, at least in part due to features of the blood-brain barrier and the unique brain microenvironment.<sup>3</sup> Fortunately, targeted therapies (TTs) and immune checkpoint inhibitors (ICIs) have shown a beneficial effect on intracranial disease response and survival in patients with BMs of certain cancer types, for example in subgroups of melanoma and non-small cell lung cancer.<sup>4,5</sup> Local therapies, such as surgical resection and stereotactic radiosurgery (SRS), have also improved over the past years and are now increasingly applied. Currently, SRS is even found effective in patients with over 10 brain lesions.<sup>6,7</sup>

The increased use of these systemic and local treatments results in an increased incidence of treatment-related effects. Pseudoprogression (PsPD) is a commonly used term to describe such effects, but its definition is highly variable in the literature.<sup>8</sup> In general, PsPD is defined as an increase of radiological abnormalities, months after therapy, which is not actual tumour progression.<sup>8</sup> Pseudoprogression can be found after treatment with SRS or systemic treatment such as ICIs.<sup>9</sup> Radiation necrosis (RN), which can appear as pseudoprogression on imaging, is a treatment-related effect confirmed by histopathology, found months to years after treatment with SRS. It can lead to invalidating neurological symptoms or even death.<sup>8,10</sup>

As a result of these new developments, these days, treating physicians face a number of questions. With the rising incidence of BMs, what is the right time to screen for BMs in patients with cancer and is screening even effective (Figure 1a)? When BMs have emerged, how extensive are they, and how can BMs be differentiated from other intracranial lesions (Figure 1b)? Finally, how can treatment best be planned (Figure 1c) and monitored (Figure 1d)?

Figure 1. The role of clinical imaging in brain metastasis management. A, B, C and D represent separate sections in this review.



In answering these questions, imaging plays an increasingly important role; in fact, it already is the cornerstone in clinical decision making for oncology today. In this review, we describe the application of several imaging techniques in the clinical practice of BM management, and the promising new developments that lie ahead.

## SCREENING FOR BRAIN METASTASES

### Incidence and timing

The incidence of BMs has increased over the past decade. The aging population leads to a yearly increase in cancer diagnoses, which in turn increases the probability of BMs.<sup>11,12</sup> Further adding to that probability are the improved systemic disease control that modern treatments provide, along with more frequent use of sensitive imaging techniques.<sup>3,13</sup> The lifetime incidence to develop BMs for a patient with cancer lies approximately between 10 and 30%, but might be even higher due to selection bias in reported studies.<sup>3,13,14</sup>

Not only the incidence of BMs has increased over time but also the interval between primary tumour diagnosis and BM development.<sup>12</sup> This shift in disease course might be another result of improved systemic treatments.

Substantial geographical variations in the application of diagnostics, access to health care and health care/economic policies make it difficult to know the exact incidence of BMs. Asymptomatic BMs are only detected by screening or by autopsy after death. The presence of extracranial metastatic disease, especially metastases in liver and lungs, increases the likelihood of BMs in patients with any cancer type.<sup>3</sup> Furthermore, certain primary tumours and molecular characteristics are associated with a higher risk of BMs.<sup>3</sup> Lung cancer, breast cancer and melanoma are most often associated with BMs, but gastro-intestinal cancer, renal cell cancer and gynaecologic cancers are also increasingly

found to metastasise to the brain.<sup>3,13,15</sup> Table 1 provides more in-depth information on BMs per tumour type.

### To screen or not to screen

Imaging of the brain in oncological patients with neurological deficits or symptoms of increased intracranial pressure (*e.g.*, headache, vomiting) is routinely performed to assess the presence of BMs. However, there is no consensus on screening for asymptomatic BMs, not even for cancer types with high risk of BMs. For example, the European Society for Medical Oncology (ESMO) recommends screening for BMs in all patients with NSCLC, whereas the National Comprehensive Cancer Network (NCCN) does not recommend screening in stage I NSCLC patients without symptoms suggestive of BMs.<sup>20</sup> A survey among treating physicians across the world showed that 85% of the respondents performed screening of BMs at primary presentation of advanced lung cancer in patients without symptoms.<sup>34</sup> In SCLC, screening for BMs is always recommended at primary diagnosis.<sup>35</sup> For patients with melanoma, the NCCN recommends screening in patients with stage IIIC to IV, whereas in breast cancer, screening is only recommended for symptomatic patients.<sup>36</sup>

Arguments against screening are that BMs can develop much later in the disease course and could therefore be missed by screening “too early”. In addition, it is not known how fast asymptomatic BMs become symptomatic, which could be within a short time interval; in that case, symptomatology would soon have been followed by imaging anyway. Moreover, it is not yet known whether early detection of asymptomatic BMs truly impacts treatment decisions and improves survival.<sup>28,37</sup>

Arguments in favour of screening are that, with knowledge of asymptomatic BMs, treating physicians can make better informed decisions about systemic treatments. Potentially,

Table 1. Primary tumours associated with brain metastases (BMs)

<p><b>Lung cancer</b></p> <ul style="list-style-type: none"> <li>• Second highest incidence in the general population<sup>15</sup></li> <li>• Two-thirds of patients with BMs as a first diagnosis have lung cancer.<sup>15-17</sup></li> <li>• Non-small cell lung cancer (NSCLC) constitutes 85% of all lung cancer types; small cell lung cancer (SCLC) has the highest risk of BMs<sup>15</sup></li> <li>• Reported lifetime risk of BM development<sup>16</sup>: <ul style="list-style-type: none"> <li>• 19.9% in all disease stages</li> <li>• 9.2% in local disease</li> <li>• 14.6% in regional disease</li> <li>• 29.9% in metastatic disease</li> </ul> </li> <li>• Risk factors for BMs: younger age, female gender, adenocarcinoma subtype, and more advanced disease (both locoregional and metastatic).<sup>17-19</sup></li> <li>• Driver mutations for targeted therapy: endothelial growth factor receptor (EGFR) mutations in 30-70% and anaplastic lymphoma kinase (ALK) mutations in 60-90% of BMs from NSCLC<sup>3,20,21</sup></li> </ul>
<p><b>Breast cancer</b></p> <ul style="list-style-type: none"> <li>• Highest incidence in the general population<sup>22</sup></li> <li>• BMs can develop late in the disease course<sup>23</sup></li> <li>• Reported lifetime risk of BMs<sup>16</sup>: <ul style="list-style-type: none"> <li>• 5.1% in all disease stages</li> <li>• 2.5% in local disease</li> <li>• 6.8% in regional disease</li> <li>• 14.2% in metastatic disease</li> </ul> </li> <li>• Risk factors for BMs: age above 41 years, triple-negative and human epidermal growth factor receptor 2 (HER2)-positive subtypes, and metastatic disease in 2-3 extracranial sites<sup>3,23</sup></li> <li>• Driver mutations for targeted therapy: HER2-positive BMs<sup>24</sup></li> </ul>
<p><b>Melanoma</b></p> <ul style="list-style-type: none"> <li>• Highest risk to metastasise to the brain of all solid tumours<sup>15</sup></li> <li>• Approximately half of melanoma patients have BMs in their disease course<sup>15</sup></li> <li>• BMs can occur very late in the disease course, even more than 10 years after initial diagnosis<sup>8,25</sup></li> <li>• Reported lifetime risk of BMs:<sup>16</sup> <ul style="list-style-type: none"> <li>• 6.9% in all disease stages</li> <li>• 4.1% in local disease</li> <li>• 18.5% in regional disease</li> <li>• 36.8% in metastatic disease</li> </ul> </li> <li>• Risk factors for BMs: older age (peak incidence between 50-59 years), male gender, specific characteristics of the primary melanoma (higher T-stage, location at head/neck or trunk, presence of ulceration, nodular subtype, desmoplastic or spindle cell melanoma, increasing depth of invasion)<sup>3,26,27</sup></li> <li>• Driver mutations for targeted therapy: V-raf murine sarcoma viral oncogene homolog B1 (BRAF) mutations are found in approximately half of melanoma patients with BMs (not specifically associated with a higher risk for BMs)<sup>26-28</sup></li> </ul>
<p><b>Renal cell cancer (RCC)</b></p> <ul style="list-style-type: none"> <li>• Low incidence in the general population, metastasises to the brain relatively often<sup>29</sup></li> <li>• Reported lifetime risk of BMs<sup>6,16</sup>: <ul style="list-style-type: none"> <li>• 6.5% in all disease stages</li> <li>• 2.5% in local disease</li> <li>• 7.6% in regional disease</li> <li>• 13.4% in metastatic disease</li> </ul> </li> <li>• Clear cell RCC most common subtype associated with BMs<sup>3,29</sup></li> <li>• Driver mutations for targeted therapy: vascular endothelial growth factor receptor (VEGFR)<sup>39</sup></li> </ul>

(Continued)

Table 1. (Continued)

<p><b>Colorectal cancer (CRC)</b></p> <ul style="list-style-type: none"> <li>• Most frequent type of gastro-intestinal cancer; in the top 5 of general population cancer incidence<sup>6,22,30</sup></li> <li>• Reported lifetime risk of BMs<sup>16,24</sup>: <ul style="list-style-type: none"> <li>• 1.8% in all disease stages</li> <li>• 0.8% in local disease</li> <li>• 2.0% in regional disease</li> <li>• 2.9% in metastatic disease</li> </ul> </li> <li>• CRC rarely metastasises to the brain, usually late in the disease course<sup>30</sup></li> <li>• Driver mutations for targeted therapy: RAS mutations<sup>31</sup></li> </ul>
<p><b>Gynaecological cancers</b></p> <ul style="list-style-type: none"> <li>• Incidence of BMs is low (&lt;1%)<sup>32</sup></li> <li>• Most common types associated with BMs are ovarian, endometrial and cervical cancer<sup>32</sup></li> <li>• Data on BMs of gynaecological cancers is limited<sup>33</sup></li> </ul>

there are also more local treatment options: asymptomatic BMs tend to be smaller and therefore better to treat by surgery or radiation. In general, screening for BMs is considered in more advanced disease stages. In case of extracranial metastatic disease, screening for BMs should be considered if BMs would change the treatment plan. In cancers that rarely metastasise to the brain, such as renal cell, colorectal and gynaecologic cancers, screening is generally only performed in patients with symptoms and/or neurologic deficits.

## DIAGNOSING BRAIN METASTASES

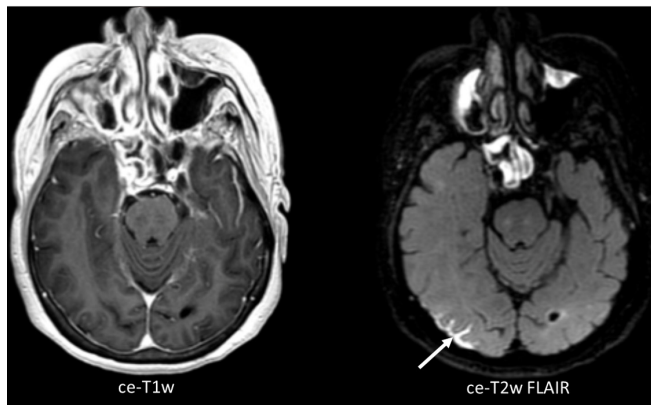
Since screening for BMs is not standard of care, most patients with BMs will present with symptoms such as headache, nausea or vomiting, epilepsy or neurologic deficits. In the acute setting, computed tomography (CT) is usually performed for rapid intracerebral evaluation and detection of potential neurosurgical emergencies.<sup>38</sup> CT is also a useful tool to detect haemorrhage, calcification, and evaluate osseous structures.<sup>39</sup> The golden standard for detecting BMs, however, is magnetic resonance imaging (MRI).<sup>3,14</sup> This imaging technique has excellent soft-tissue contrast with high-resolution depiction of tissue anatomy.<sup>40</sup>

### Conventional MRI

In order to achieve a more reliable inter-image, and inter-centre, assessment of BMs at diagnosis and in treatment evaluation, Kaufmann et al have proposed a standardised MRI protocol.<sup>14</sup> Their recommendation is based on that of the working group of Response Assessment in Neuro-Oncology-Brain Metastases (RANO-BM) and the Brain Tumour Imaging Protocol for glioma research (BTIP).<sup>14</sup> According to this standard protocol, a pre- and post-contrast 3D T1W sequence is always required.<sup>14</sup> Furthermore, high-resolution T2W imaging should be performed, optionally with fluid attenuation inversion recovery (FLAIR) to optimally detect vasogenic oedema.<sup>14</sup>

In order to detect all BMs, in particular small lesions (<5 mm), MRI needs to be highly sensitive. Higher field strength increases this sensitivity; scanning at 3 Tesla (T) is much more sensitive than scanning at 1.5T.<sup>41</sup> The optimal choice of post-contrast T1W pulse sequence is still under debate. A magnetisation prepared

Figure 2. Axial, three-dimensional (3D) contrast-enhanced T1W image (ce-T1W) on the left, with the corresponding 3D contrast-enhanced T2W Fluid Attenuated Inversion Recovery image (ce-T2W FLAIR) on the right, from a patient with leptomeningeal disease (LMD, arrow). The ce-T2W FLAIR image shows the region of LMD much clearer than the ce-T1W image



(“IR-prepped”) gradient recalled echo (GRE) pulse sequence is robust, has high signal-to-noise, and is widely available.<sup>14</sup> Kaufmann et al recommend this sequence to be in the minimal standardised MRI protocol for BMs.<sup>14</sup> However, IR-GRE sequences have slightly less conspicuous contrast enhancement than spin echo (SE) or turbo SE (TSE)-based pulse sequences, in particular at lower field strengths (<3T).<sup>14</sup> 3D (T)SE sequences are however less widely available and have only been sufficiently evaluated at 3T, while 2D sequences render the technique less sensitive to small lesions due to lower through-plane resolution. While the “ideal” protocol thus replaces IR-GRE with 3D TSE T1W imaging pre- and post-contrast administration, and is best performed at 3T, this is not universally attainable. Some sites therefore add a (T)SE sequence to the protocol, but this clearly comes at the cost of additional scanning time.<sup>14</sup> Double or triple doses of a gadolinium-based contrast agent (GBCA) are superior to a single dose, but can lead to an increased number of false-positive findings.<sup>3,38</sup> For the detection of dural or leptomeningeal disease, contrast-enhanced 3D MRI is the most sensitive technique, especially combined with FLAIR (Figure 2).<sup>38</sup> Time-delayed imaging, for example, waiting 15 to 20 min before scanning post-contrast, may further increase sensitivity, especially in the posterior circulation.<sup>38</sup> However, this is time-consuming and therefore not always possible in clinical practice.<sup>38</sup>

Brain metastases are usually iso- to hypointense to grey matter on T1W images, and are of variable intensity on T2W images.<sup>38</sup> Vasogenic oedema typically involves the white matter, creating a “finger-shaped” lineage below the cortex.<sup>38</sup> This oedema can be strikingly disproportionate to the size of the BM, but it can also be completely absent.<sup>3</sup> Other common features of BMs are a spherical, delineated shape and ring enhancement of larger BMs after contrast administration, due to central necrosis.<sup>38,42</sup> Calcification in BMs can be of high intensity on T1W and low on T2W imaging, but varies with its composition.<sup>38</sup> Haemorrhage in BMs can show varying signal intensities on T1W and T2W imaging, depending on different stages over time.<sup>38</sup> Because BMs spread

haematogenically, they usually occur on the grey-white matter junction or watershed zones, where the luminal diameters of arterioles decrease.<sup>3,14</sup> Most BMs are found supratentorially (80%), but BMs can also emerge below the tentorium.<sup>14</sup> More features per primary tumour type are displayed in Table 2; however, none of these features are completely specific for BMs or for BMs of different primaries. The differential diagnosis includes infection (abscess in particular), inflammation, auto-immune disease and primary brain tumour.<sup>3</sup>

#### Additional imaging

In addition to the standard MRI protocol, advanced MRI sequences and other imaging techniques may provide information on specific lesion characteristics. Although they are promising for clinical imaging, most of these techniques are still evaluated in experimental settings and lack standardisation across centres.

Susceptibility weighted imaging (SWI) might be of added value in confirming the diagnosis of melanoma BMs.<sup>45</sup> Melanin and blood products can be found in these lesions and are paramagnetic, showing susceptibility artefacts on SWI.<sup>45</sup> Since approximately 66% of melanoma BMs have such susceptibility-related signal loss, SWI might be used to differentiate BMs of melanoma from other cancer types.<sup>45</sup> In general, however, SWI is not sufficiently sensitive for detecting BMs.<sup>38</sup> A small study investigated the use of quantitative susceptibility mapping (QSM) to detect melanin content in melanoma BMs, but could not demonstrate an isolated signal for melanin.<sup>47</sup>

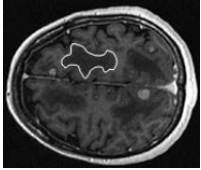
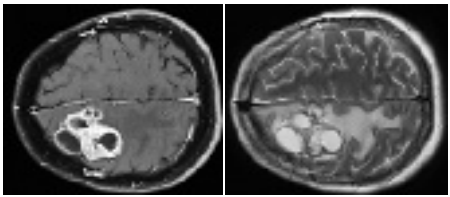
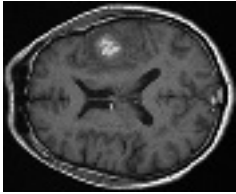
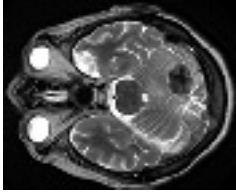
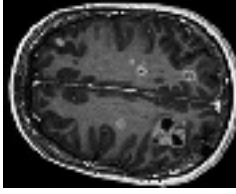
DWI can show signal decreases (restriction) in BMs due to increased cellularity.<sup>38</sup> This sequence is most commonly used to differentiate BMs from other intracranial lesions as abscess. Both BMs and abscesses can present as a ring-enhancing lesion on post-contrast T1W imaging.<sup>3,40</sup> In abscesses, diffusion is usually far more restricted than in BMs, particularly in the central non-enhancing portion. However, brain abscesses can rarely (4%) also present without diffusion restriction.<sup>3,38</sup>

Since increased tissue perfusion is a hallmark of cancer, perfusion MRI can be used to discriminate BMs from normal brain tissue. Dynamic susceptibility contrast (DSC) perfusion MRI is most commonly used and measures relative cerebral blood volume (rCBV). Arterial spin labelling (ASL), measuring cerebral blood flow (CBF), is less commonly used. It has a relatively lower signal-to-noise ratio and spatial resolution, but also has advantages over DSC: there is no need for exogenous contrast administration, it is not sensitive to susceptibility artefacts or signal drop (with an SE read-out) and it does suffer from leakage effects.<sup>48</sup> Perfusion MRI could help to distinguish BMs from primary brain tumours: the peritumoural region of glioblastoma is mostly associated with higher rCBV values than that of BMs.<sup>49</sup> Unfortunately, however, lack of standardisation within and between centres still results in undefined cut-off points for rCBV and CBF for diagnosing different aetiologies.<sup>38</sup>

Metabolic information can be obtained with magnetic resonance spectroscopy (MRS). Using the standardised (Cho)/Creatine



Table 2. Imaging features of BMs, characteristic (but not specific) for different primary tumours

Primary tumour type	Lung cancer	Breast cancer	Melanoma	Renal cell cancer	Colorectal cancer	Gynaecological cancers
<p><b>Common imaging features</b></p> <ul style="list-style-type: none"> <li>Common presentation with multiple BMs<sup>1,5,38</sup></li> <li>Associated with leptomeningeal disease, especially adenocarcinoma<sup>3,43</sup></li> </ul>	<ul style="list-style-type: none"> <li>A single or multiple BMs<sup>38</sup></li> <li>Associated with leptomeningeal disease<sup>3</sup></li> <li>Triple negative breast cancer can show substantially more necrotic and cystic BMs, with very bright T2W signal and low T1W signal centrally<sup>3,38</sup></li> </ul>	<ul style="list-style-type: none"> <li>Common presentation with multiple BMs<sup>15,27,38,44</sup></li> <li>Associated with leptomeningeal disease<sup>3</sup></li> <li>Haemorrhagic lesions are common<sup>45</sup></li> <li>Commonly hyperintense on native T1W imaging due to haemorrhage and/or melanin<sup>3,45</sup></li> </ul>	<ul style="list-style-type: none"> <li>A single BM is diagnosed in &gt; 50% of cases<sup>29,38</sup></li> <li>Associated with spontaneous haemorrhage<sup>29</sup></li> </ul>	<ul style="list-style-type: none"> <li>A single or multiple BMs<sup>38</sup></li> <li>Can present as mucinous or protein-rich lesions, with low T2W signal intensity<sup>38</sup></li> </ul>	<ul style="list-style-type: none"> <li>A single or multiple BMs<sup>46</sup></li> </ul>	
MRI example	 <p>Axial contrast-enhanced T1W: multiple BMs and vasogenic oedema (one zone is highlighted by the white delineation).</p>	 <p>Top: axial pre-contrast T1W: revealing BMs through increased signal intensity (melanin). Bottom: axial contrast-enhanced T1W: revealing even more contrast-enhancing BMs in the same patient.</p>	 <p>Axial pre-contrast T1W: a single BM with signal hyperintensity, suggestive of blood products.</p>	 <p>Axial pre-contrast T2W: BM in the left cerebellar hemisphere with low (central) signal intensity.</p>	 <p>Axial contrast-enhanced T1W: multiple BMs from ovarian carcinoma.</p>	

(Cr)-ratio, MRS might help to distinguish non-small cell lung cancer (NSCLC) from melanoma and breast cancer BMs.<sup>50</sup> In a study by Huang *et al*, a ratio < 2.0 was never found in melanoma BMs, in 38% of patients with lung cancer BMs and in 24% of patients with breast cancer BMs.<sup>50</sup> A high lipid content measured with MRS is associated with BMs from colorectal cancer.<sup>38</sup> In clinical practice, MRS is not widely used due to challenges in acquisition, time constraints and limited availability of analysis tools on commercial MR scanners.<sup>51</sup>

Combining positron emission tomography (PET) with CT or MRI combines metabolic with anatomic information. Numerous tracers have been tested in small, selected patient groups. [<sup>18</sup>F]-2-fluoro-2-deoxy-D-glucose (<sup>18</sup>F-FDG) is most widely used in general oncological practice and has high uptake in tumour cells, but the diagnostic accuracy for detecting BMs is limited since the brain itself also has high uptake of <sup>18</sup>F-FDG.<sup>9</sup> [<sup>52</sup>Ga]Gadododecane tetra-acetic acid-fibroblast activation protein inhibitor (DOTA-FAPI)-04 is a relatively new tracer, which was found to have a higher efficacy than <sup>18</sup>F-FDG in PET/CT imaging in detecting brain tumours.<sup>53</sup> Radiolabelled amino acids are also more suitable for imaging pathology in the brain than <sup>18</sup>F-FDG, since these tracers have low uptake in normal brain tissue.<sup>9</sup> [<sup>11</sup>C]-methyl-L-methionine (MET), 3,4-dihydroxy-6-[<sup>18</sup>F]-fluoro-L-phenylalanine (<sup>18</sup>F-FDOPA) and O-(2-[<sup>18</sup>F]-fluoroethyl)-L-tyrosine (<sup>18</sup>F-FET) are recommended for detecting BMs, with high uptake values indicating overexpression of L-type amino acid transporter (LAT), a feature of BMs.<sup>9</sup>

The specific combination of PET with MRI is being implemented in clinical use but still has some relevant technical challenges to overcome. The synergy of combined MRI and PET could help to improve the diagnostic value of both modalities.<sup>54</sup>

## TREATING BRAIN METASTASES

### Local therapies

Surgical resection is usually performed in patients with relatively good performance status, stable or absent systemic disease, and one of two intracranial scenarios: either up to three BMs, or a single BM amongst several smaller, presumably asymptomatic lesions.<sup>55,56</sup> Resected BMs are usually symptomatic or expected to become symptomatic soon. In rare cases, the brain is the only site of metastatic disease, in which case resection could even have curative intention. Surgical resection is sometimes primarily performed for diagnosis rather than treatment; for example, when the primary tumour is unknown or when there is a differential diagnosis (such as glioma or abscess).

The goal of resection is always to remove a BM in its entirety. To achieve complete resection, intraoperative imaging and surgical techniques are constantly being improved, requiring accurate cross-sectional imaging for neuronavigation.<sup>55</sup> Fluorescence-guided surgery with 5-aminolevulinic acid (5-ALA), best known for glioma resection, is less frequently used in BM resections, mostly in non-academic centers.<sup>57</sup> Intraoperative ultrasound (US) is frequently used in surgery, providing a real-time and inexpensive method that distinguishes the dense tissue of BMs from normal brain tissue.<sup>55,57</sup> The use of intra-operative MRI

systems is still limited due to lacking cost-effectiveness; CT is not useful due to shortcomings in depicting soft tissue contrast.<sup>55,57</sup>

Laser interstitial thermal therapy (LITT) uses laser ablation and is increasingly explored for local BM treatment.<sup>58</sup> This technique uses pre- and intra-treatment MRI guidance to plan the laser probe tract and to adjust treatment during the procedure.<sup>58</sup> During ablation, changes in MRI signal, in particular T1W hyperintensity, provide information on the laser-induced tissue damage.<sup>58</sup>

Early postoperative imaging, preferably with MRI, to determine the completeness of surgical resection, should be performed within 48 up to 72 h after surgery to avoid surgery-related enhancement.<sup>57</sup> In case of residual tumour in the resection cavity, adjuvant SRS is increasingly routinely performed.<sup>56,59</sup>

Whole brain radiotherapy (WBRT) was historically the treatment of choice for patients with multiple BMs.<sup>7</sup> Stereotactic radiosurgery (SRS) is gradually taking over this position, with recent advances that have increased effectivity and reduced toxicity, even in patients with multiple BMs.<sup>7</sup> For planning of SRS, MRI including at least a post-contrast 3D T1W sequence is required to accurately visualise the BMs. This scan must be obtained preferably within one and ultimately within 2 weeks before the start of SRS.<sup>7,60</sup> In addition, a CT scan, preferably post-contrast and with 1-mm slice thickness, is fused with the MR images.<sup>7</sup> This CT scan is required for positioning and to correct for geographic distortions in the MR image.<sup>7</sup> Repeated MRI scans during more prolonged fractionated SRS schemes should be considered, as target volume can change during the course of therapy.<sup>60</sup>

Over half of patients treated with SRS develop BMs at other brain sites during follow-up. For this reason, regular MRI follow-up is recommended in patients who have remaining treatment options.<sup>7</sup> Follow-up MRI should be planned at intervals of 2 to 3 months; more frequent scanning does not affect clinical outcomes in the absence of neurological symptoms.<sup>7,61</sup>

### Systemic therapies

Systemic therapy is considered in all patients with metastatic disease. Systemic therapy is used in patients with asymptomatic BMs or BMs controlled by local treatment to treat active extracranial disease. However, systemic therapy can also be used to treat patients with rapid progression of BMs, when a fast response from systemic therapy can be expected. An example of the latter is the use of BRAF/MEK inhibition in melanoma patients with BMs.<sup>62</sup>

Intracranial response evaluation is required after initiation of systemic therapy. For example, in NSCLC, response evaluation of anti-PD-1 therapy is recommended after 2 to 3 months of therapy.<sup>43</sup> For sequential response evaluation, the MRI protocol should include the same sequences and sequence settings as at baseline and is preferably performed on the same scanner. For BMs, the RANO group has proposed recommendations for evaluation (RANO-BM criteria) and follow-up after ICI treatment (iRANO criteria).<sup>63,64</sup> According to the RANO-BM criteria,

diameters of up to 5 BMs are unidimensionally measured and summed. Progression is defined as this sum exceeding 20% increase compared to that on baseline MRI or the MRI showing the best response. Response to treatment is defined as a reduction of the sum by more than 30% compared with baseline.<sup>64</sup> For immunotherapy, in case of significant clinical deterioration (not caused by comorbidity/medication toxicity) within 6 months of the last treatment, a repeated MRI of the brain must be obtained 3 months following the initial MRI suspect for progression, to determine true progression.<sup>63</sup> If clinical deterioration occurs more than 6 months after the last immunotherapy treatment, the standard RANO-BM criteria apply.<sup>64</sup>

### Treatment-related effects

During follow-up, the increase of radiologic abnormalities or enhancement in the tumour region can represent BM progression or PsPD.<sup>9,40</sup> However, conventional MRI is not capable of distinguishing PsPD from true progression.<sup>8</sup> In addition, an increase in lesion volume may consist of a mixture of tumour progression and RN, making the interpretation of imaging findings even more complex.<sup>65</sup> Initial increase of imaging abnormalities such as enhancement, followed by a decrease on follow-up imaging over a clinically relevant period of time (*e.g.*, 3–6 months), should be regarded as PsPD, whereas further increase indicates true progression.<sup>8,66</sup>

Both TTs and especially ICIs are associated with PsPD, alone or in combination with SRS.<sup>9</sup> In the first weeks, up to 6 months following treatment, an inflammatory reaction can appear on MRI as an increase of contrast enhancement in both existing lesions and in newly detected lesions.<sup>9</sup> Pseudoprogression has been reported in up to 5–10% of patients treated with ICIs.<sup>9</sup>

Radiation necrosis can emerge months to years after SRS. Due to variations in applied definition of RN and uncertainty of the diagnosis, the reported incidence rates vary.<sup>8</sup> In a large,

retrospective study, Kohutek et al have reported RN to develop in  $\geq 25\%$  of BMs treated with SRS.<sup>67</sup>

Of all advanced imaging techniques, perfusion MRI is most commonly applied in clinical practice to discriminate BM progression from PsPD/RN. Relative CBV, as obtained with DSC perfusion MRI, is commonly higher in tumour than in RN due to higher vascularity of BMs.<sup>68</sup> However, optimal cut-off levels for rCBV are difficult to determine, and reported rCBV cut-off points vary across studies, while the literature on BMs – compared to that of primary brain tumours – is scarce.<sup>68–70</sup> Knitter et al evaluated interval changes in several imaging parameters and found this potentially more reliable in predicting the final diagnosis.<sup>71</sup> Taunk et al found the volume transfer constant ( $K^{\text{trans}}$ ) as obtained with DCE perfusion MRI to also be a potentially valid biomarker for predicting response following SRS.<sup>72</sup> Similar findings are reported for ASL (Figure 3)<sup>48</sup>; however, as the signals derived from these different perfusion modalities are obtained using different techniques, sometimes they might show contradicting (or complementary) results. (Figure 4).

On DWI, ADC is usually low in tumour tissue and high in RN, although this distinction is not universal.<sup>73</sup> Using MRS, Cho/Cr-ratio and Cho/N-acetyl-aspartate (NAA)-ratio were found to be higher in tumour than in RN.<sup>74</sup> In MET-PET, uptake is usually higher in progressive BMs than in RN; FDOPA- and FET-PET have also shown a potential discriminating ability in smaller studies.<sup>10,75,76</sup> Larger, multi-centre, randomized cohort studies are required for all these techniques, to determine their true clinical value.

### FUTURE PERSPECTIVES

Although research on BM diagnostics is increasing, the explorative nature of these studies limit clinical implementation.<sup>77</sup> Nevertheless, some of these techniques show promise and pave the way for future translational studies.

Figure 3. Axial contrast-enhanced T1W (ce-T1W) and native T1W images and a cerebral blood flow (CBF) map derived from arterial spin labelling (ASL), from a patient with a brain metastasis in the left parietal lobe, treated with stereotactic radiosurgery (SRS). The lesion increased in size 1 month after SRS and was histopathologically confirmed to be a combination of subacute haemorrhage and tumour progression. Most of the lesion is hyperintense before contrast administration, due to subacute haemorrhage. This portion has no perfusion on ASL. One small component is enhancing and shows increased perfusion on ASL (arrow), consistent with tumour progression.

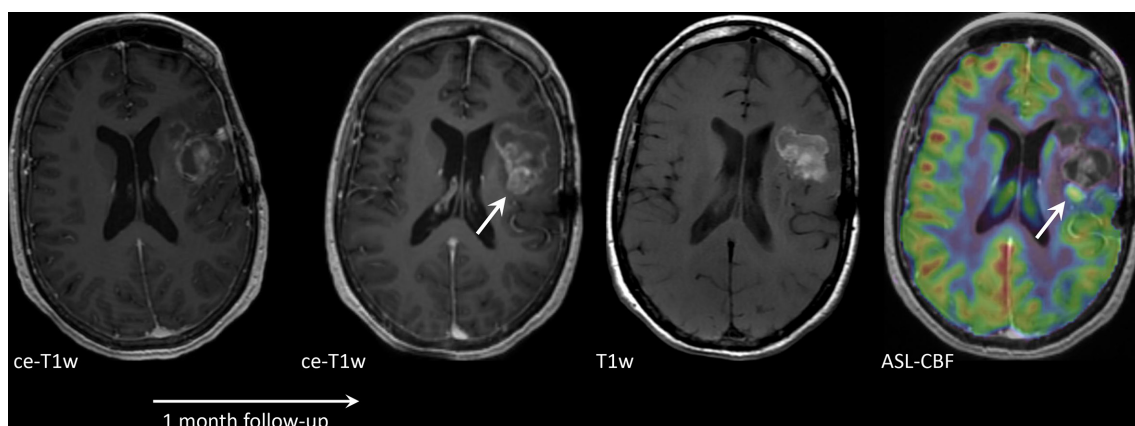
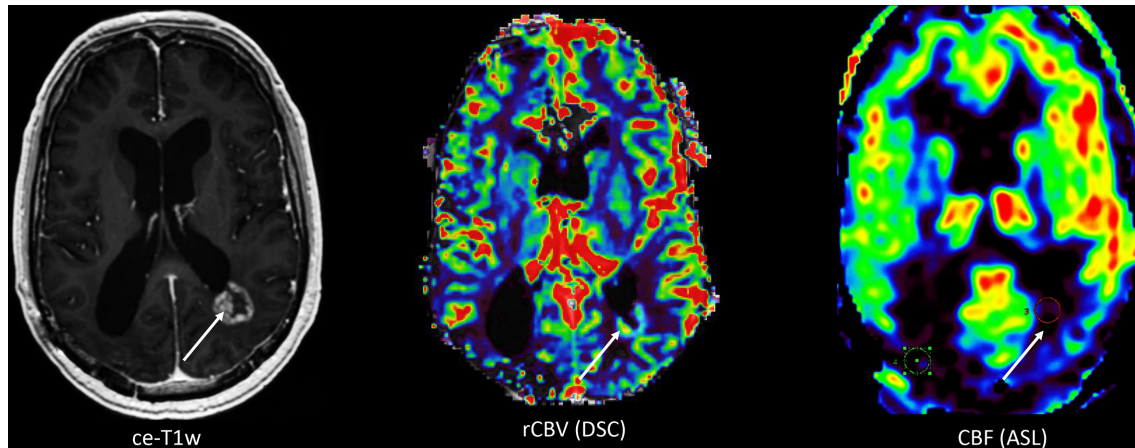




Figure 4. Axial contrast-enhanced T1W (ce-T1W) image, relative cerebral blood volume (rCBV) and cerebral blood flow (CBF) maps derived from dynamic susceptibility contrast enhanced (DSC) performed after a pre-load bolus with leakage correction and arterial spin labelling (ASL), respectively, from a 55-year-old male patient with a history of lung cancer and brain metastasis which was treated with high-dose radiation therapy. The ce-T1W image shows a ring-enhancing lesion adjacent to the left lateral ventricle with a waxing and waning course over time, suspicious of radiation necrosis. However, the lesion remained suspicious for metastasis recurrence due to the high rCBV as measured with DSC. CBF however is low, which is more consistent with the clinical diagnosis and time course of radiation necrosis. The discrepancy between findings with DSC and ASL is presumably due to leakage effects in the DSC images resulting in incorrect estimation of rCBV.



### Radiomics and biomarkers

Quantitative imaging is an upcoming field in radiology research. The ability to detect and determine the magnitude of a signal change may help to differentiate between aetiologies in tissue of interest.

Radiomics uses the quantitative features from segmented images that are difficult or even impossible to detect by visual inspection, in order to find associations with clinically relevant outcomes.<sup>78</sup> Machine- and deep-learning techniques facilitate radiomics, by automatically extracting high-dimensional features from original images and learning to recognise characteristic patterns of pathology.<sup>79</sup> In BMs, radiomics has been evaluated to determine primary tumour type and mutational status, but also to evaluate tumour response after treatment.

Kniep et al used radiomics to determine the primary tumour type of BMs; melanoma and SCLC were well recognized by their model (area under the curve [AUC] of 0.80 and 0.74, respectively), but breast cancer and NSCLC were less well differentiated (AUC 0.61 and 0.63, respectively), which could be explained by the heterogeneity of BM characteristics in these types.<sup>80</sup> Park et al used radiomics to determine NSCLC subtypes: DTI and conventional post-contrast T1W imaging could potentially detect the EGFR mutational status in BMs from NSCLC.<sup>81</sup>

In treatment surveillance, radiomics is also widely studied. Peng et al retrospectively studied conventional and, when available, perfusion MRI of 66 patients with 82 BMs that showed a volume increase following SRS.<sup>78</sup> They compared radiomics obtained with machine learning with histopathologic diagnosis. Their model showed a promising accuracy for differentiation of true progression and RN, with an AUC of 0.81.<sup>78</sup> Two other studies also assessed radiomic models in predicting response after SRS

and found similar AUCs.<sup>82,83</sup> Lee et al used radiomics to assess intratumoural heterogeneity following SRS treatment.<sup>65</sup> They identified several potential imaging parameters, such as solid, low-enhancing regions and nonviable tissue regions (e.g., non-enhancing T2 hyperintensity), to have a predictive power for tumour progression.<sup>65</sup> However, their work needs to be interpreted with caution due to several assumptions and lack of standard histopathological confirmation.<sup>65</sup>

Galldiks et al retrospectively investigated quantitative values from <sup>18</sup>F-FET-PET imaging in the follow-up of 40 patients with BMs after TT or ICI treatment.<sup>84</sup> Uptake of <sup>18</sup>F-FET in BMs was promising in differentiating between progression and PsPD after TT or ICI treatment. Also, <sup>18</sup>F-FET-PET showed promise in predicting response to treatment.

Since radiomics could provide information on specific tumour and treatment-related features, it is a promising tool to eventually obviate histopathological diagnosis or verification. However, straightforward, clinically “easy-to-interpret” biomarkers are limited as studies generally use indirect measures such as survival to estimate the implications of a biomarker, while at the same time accuracy requires further improvement.<sup>77</sup>

Although survival might not be the ideal reference standard for validating biomarkers, it is important to be able to estimate prognosis of individual patients. A clinically used and validated prognostic index, created by Sperduto et al, is the Graded Prognostic Assessment (GPA).<sup>85</sup> It combines clinical and molecular prognostic factors to predict prognosis of individual patients with BMs. Zakaria et al combined ADC values of DWI-MRI with existing survival prediction models such as the GPA.<sup>86</sup> Higher tumour ADC at initial BM diagnosis was associated with longer survival, and implementation of ADC values in the existing



models increased the accuracy of these models in predicting prognosis.

### Endogenous MRI contrasts

New imaging techniques are constantly being developed. Chemical Exchange Saturation Transfer (CEST) is a technique assessing the concentrations of large molecules such as proteins (amide proton transfer, or APT-CEST) and glucose (glucoCEST).<sup>52</sup> Since BMs have both a higher protein concentration and higher rates of glucose metabolism than normal brain, these techniques are promising for detecting and characterising BMs.

Like CEST, new imaging techniques that provide contrast from endogenous molecules might substitute exogenous contrast agents such as GCBAs. An example is the replacement of DSC-MRI, for which commonly an increased dose of GBCA is used, with non-invasive perfusion imaging techniques. Vu et al demonstrated the use of blood-oxygen-level-dependent (BOLD) MRI, in which transient hypoxia was used to generate contrast.<sup>87</sup>

### Optimised treatment delivery

Theranostics combines the diagnostic and therapeutic properties of radiolabelled compounds.<sup>88</sup> In the central nervous system, most theranostics were investigated in glioma. In BMs, the anti-prostate-specific membrane antibody (PSMA) is promising for theranostics. PSMA can be radiolabelled for both diagnosis using PET (Gallium 68 [<sup>69</sup>Ga]-PSMA) and radionuclide therapy with Lutetium-117 [<sup>117</sup>Lu]Lu-PSMA-617 and Actinium-225 [<sup>225</sup>Ac]Ac-PSMA-616.<sup>89</sup> Therefore, theranostics seems to be a next step in optimised BM treatment.

The term “theranostics” is formally reserved for a single compound with both diagnostic and therapeutic abilities. However, PET tracers combined with certain compounds can also be used to predict response to treatment. An example is [<sup>89</sup>Zr]-pertuzumab,

studied in patients with breast cancer to detect human epidermal growth factor receptor 2 (HER2)-positive BMs and to determine optimal dosimetry.<sup>90</sup> Since HER2-positive BMs can be effectively treated with TT, patients can be optimally selected for this therapy. Furthermore, non-responders can be selected upfront, preventing unnecessary TT treatment and side effects.

Poor penetration of systemic drugs into BMs, due to features of the blood-brain-barrier and blood-tumour-barrier, has been a major concern limiting treatment efficacy. Focussed ultrasound has been suggested to improve drug delivery to BMs by opening the blood-brain-barrier and/or blood-tumour-barrier; this has been investigated in glioma and a small trial in patients with breast cancer BMs is currently ongoing.<sup>91</sup>

### CONCLUSION

The management of patients with BMs greatly relies on imaging. Screening for BMs is indicated in oncologic subgroups with a higher risk for BMs. However, it is still a matter of debate whether earlier detection of BMs will improve outcome. MRI is the cornerstone of diagnosis and evaluation of BMs. In discriminating BMs from other intracranial lesions or treatment-related effects, more advanced imaging techniques such as perfusion MRI and PET can be of added value. Imaging can also guide local and advanced systemic treatments with increasing precision. Current studies show promise for new imaging biomarkers and contrasts, and in finding ways to optimise treatment of BMs. Ultimately, all these research efforts aim to improve survival and quality of life for patients with BMs.

### FUNDING

S.D. is funded by a grant of the Daniel Den Hoed Foundation. The funding organisation is not involved in the content of this review paper.

### REFERENCES

- Dasgupta A, Co J, Winter J, Millar B-A, Laperriere N, Tsang DS, et al. Clinicopathologic and treatment features of long-term surviving brain metastasis patients. *Curr Oncol* 2021; **28**: 549–59. doi: <https://doi.org/10.3390/curroncol28010054>
- Hall WA, Djalilian HR, Nussbaum ES, Cho KH. Long-term survival with metastatic cancer to the brain. *Med Oncol* 2000; **17**: 279–86. doi: <https://doi.org/10.1007/BF02782192>
- Achrol AS, Rennert RC, Anders C, Soffietti R, Ahluwalia MS, Nayak L, et al. Brain metastases. *Nat Rev Dis Primers* 2019; **5**: 5. doi: <https://doi.org/10.1038/s41572-018-0055-y>
- Goldberg SB, Gettinger SN, Mahajan A, Chiang AC, Herbst RS, Sznol M, et al. Pembrolizumab for patients with melanoma or non-small-cell lung cancer and untreated brain metastases: early analysis of a non-randomised, open-label, phase 2 trial. *Lancet Oncol* 2016; **17**: 976–83. doi: [https://doi.org/10.1016/S1470-2045\(16\)30053-5](https://doi.org/10.1016/S1470-2045(16)30053-5)
- Tawbi HA, Forsyth PA, Algazi A, Hamid O, Hodi FS, Moschos SJ, et al. Combined nivolumab and ipilimumab in melanoma metastatic to the brain. *N Engl J Med* 2018; **379**: 722–30. doi: <https://doi.org/10.1056/NEJMoa1805453>
- Niranjan A, Monaco E, Flickinger J, Lunsford LD. Guidelines for multiple brain metastases radiosurgery. *Prog Neurol Surg* 2019; **34**: 100–9. doi: <https://doi.org/10.1159/000493055>
- Hartgerink D, Swinnen A, Roberge D, Nichol A, Zygmanski P, Yin F-F, et al. LINAC based stereotactic radiosurgery for multiple brain metastases: guidance for clinical implementation. *Acta Oncol* 2019; **58**: 1275–82. doi: <https://doi.org/10.1080/0284186X.2019.1633016>
- Thust SC, van den Bent MJ, Smits M. Pseudoprogression of brain tumors. *J Magn Reson Imaging* 2018; **48**: 571–89. doi: <https://doi.org/10.1002/jmri.26171>
- Galldiks N, Kocher M, Cecon G, Werner J-M, Brunn A, Deckert M, et al. Imaging challenges of immunotherapy and targeted therapy in patients with brain metastases: response, progression, and pseudoprogression. *Neuro Oncol* 2020; **22**: 17–30. doi: <https://doi.org/10.1093/neuonc/noz147>
- Lupattelli M, Ali E, Ingrassio G, Saldi S, Fulcheri C, Borghesi S, et al. Stereotactic radiotherapy for brain metastases: imaging

- tools and Dosimetric predictive factors for radionecrosis. *J Pers Med* 2020; **10**: 59. doi: <https://doi.org/10.3390/jpm10030059>
11. Smith BD, Smith GL, Hurria A, Hortobagyi GN, Buchholz TA. Future of cancer incidence in the United States: burdens upon an aging, changing nation. *J Clin Oncol* 2009; **27**: 2758–65. doi: <https://doi.org/10.1200/JCO.2008.20.8983>
  12. Nieder C, Spanne O, Mehta MP, Grosu AL, Geinitz H. Presentation, patterns of care, and survival in patients with brain metastases: what has changed in the last 20 years? *Cancer* 2011; **117**: 2505–12. doi: <https://doi.org/10.1002/cncr.25707>
  13. Lu-Emerson C, Eichler AF. Brain metastases. *Continuum* 2012; **18**: 295–311. doi: <https://doi.org/10.1212/01.CON.0000413659.12304.a6>
  14. Kaufmann TJ, Smits M, Boxerman J, Huang R, Barboriak DP, Weller M, et al. Consensus recommendations for a standardized brain tumor imaging protocol for clinical trials in brain metastases. *Neuro Oncol* 2020; **22**: 757–72. doi: <https://doi.org/10.1093/neuonc/noaa030>
  15. Ostrom QT, Wright CH, Barnholtz-Sloan JS. Brain metastases: epidemiology. *Handb Clin Neurol* 2018; **149**: 27–42. doi: <https://doi.org/10.1016/B978-0-12-811161-1.00002-5>
  16. Barnholtz-Sloan JS, Sloan AE, Davis FG, Vignea FD, Lai P, Sawaya RE. Incidence proportions of brain metastases in patients diagnosed (1973 to 2001) in the metropolitan Detroit cancer surveillance system. *J Clin Oncol* 2004; **22**: 2865–72. doi: <https://doi.org/10.1200/JCO.2004.12.149>
  17. Goncalves PH, Peterson SL, Vignea FD, Shore RD, Quarshie WO, Islam K, et al. Risk of brain metastases in patients with nonmetastatic lung cancer: analysis of the metropolitan Detroit surveillance, epidemiology, and end results (SEER) data. *Cancer* 2016; **122**: 1921–7. doi: <https://doi.org/10.1002/cncr.30000>
  18. Hubbs JL, Boyd JA, Hollis D, Chino JP, Saynak M, Kelsey CR. Factors associated with the development of brain metastases: analysis of 975 patients with early stage nonsmall cell lung cancer. *Cancer* 2010; **116**: 5038–46. doi: <https://doi.org/10.1002/cncr.25254>
  19. Chen S, Hua X, Jia J, Wu Y, Wei S, Xu L, et al. Risk factors for brain metastases in patients with non-small cell lung cancer: a meta-analysis of 43 studies. *Ann Palliat Med* 2021; **10**: 3657–72. doi: <https://doi.org/10.21037/apm-20-1722>
  20. Ando T, Kage H, Saito M, Amano Y, Goto Y, Nakajima J, et al. Early stage non-small cell lung cancer patients need brain imaging regardless of symptoms. *Int J Clin Oncol* 2018; **23**: 641–6. doi: <https://doi.org/10.1007/s10147-018-1254-y>
  21. Wrona A. Management of CNS disease in ALK-positive non-small cell lung cancer: is whole brain radiotherapy still needed? *Cancer Radiother* 2019; **23**: 432–8. doi: <https://doi.org/10.1016/j.canrad.2019.03.009>
  22. Cancer Statistics: World Health Organisation (WHO). 2020. Available from: <https://www.cancer.gov/about-cancer/understanding/statistics>.
  23. Martin AM, Cagney DN, Catalano PJ, Warren LE, Bellon JR, Punglia RS, et al. Brain metastases in newly diagnosed breast cancer: a population-based study. *JAMA Oncol* 2017; **3**: 1069–77. doi: <https://doi.org/10.1001/jamaoncol.2017.0001>
  24. Leone JP, Leone BA. Breast cancer brain metastases: the last frontier. *Exp Hematol Oncol* 2015; **4**: 33. doi: <https://doi.org/10.1186/s40164-015-0028-8>
  25. Osella-Abate S, Ribero S, Sanlorenzo M, Maule MM, Richiardi L, Merletti F, et al. Risk factors related to late metastases in 1,372 melanoma patients disease free more than 10 years. *Int J Cancer* 2015; **136**: 2453–7. doi: <https://doi.org/10.1002/ijc.29281>
  26. Zhang D, Wang Z, Shang D, Yu J, Yuan S. Incidence and prognosis of brain metastases in cutaneous melanoma patients: a population-based study. *Melanoma Res* 2019; **29**: 77–84. doi: <https://doi.org/10.1097/CMR.0000000000000538>
  27. Gardner LJ, Ward M, Andtbacka RHI, Boucher KM, Bowen GM, Bowles TL, et al. Risk factors for development of melanoma brain metastasis and disease progression: a single-center retrospective analysis. *Melanoma Res* 2017; **27**: 477–84. doi: <https://doi.org/10.1097/CMR.0000000000000382>
  28. Steindl A, Berghoff AS. Brain metastases in metastatic cancer: a review of recent advances in systemic therapies. *Expert Rev Anticancer Ther* 2021; **21**: 325–39. doi: <https://doi.org/10.1080/14737140.2021.1851200>
  29. Shuch B, La Rochelle JC, Klatt T, Riggs SB, Liu W, Kabbinar FF, et al. Brain metastasis from renal cell carcinoma: presentation, recurrence, and survival. *Cancer* 2008; **113**: 1641–8. doi: <https://doi.org/10.1002/cncr.23769>
  30. Bonadio RC, Freitas GF, Batista DN, Moreira OAN, Dias CAR, Castria TB, et al. Epidemiology and outcomes of patients with brain metastases from colorectal Cancer- Who are these patients? *Clin Colorectal Cancer* 2021; **20**: e195–200. doi: <https://doi.org/10.1016/j.clcc.2021.04.002>
  31. Yaeger R, Cowell E, Chou JF, Gewirtz AN, Borsu L, Vakiani E, et al. RAS mutations affect pattern of metastatic spread and increase propensity for brain metastasis in colorectal cancer. *Cancer* 2015; **121**: 1195–203. doi: <https://doi.org/10.1002/cncr.29196>
  32. Cagney DN, Martin AM, Catalano PJ, Redig AJ, Lin NU, Lee EQ, et al. Incidence and prognosis of patients with brain metastases at diagnosis of systemic malignancy: a population-based study. *Neuro Oncol* 2017; **19**: 1511–21. doi: <https://doi.org/10.1093/neuonc/nox077>
  33. Kim YZ, Kwon JH, Lim S. A clinical analysis of brain metastasis in gynecologic cancer: a retrospective multi-institute analysis. *J Korean Med Sci* 2015; **30**: 66–73. doi: <https://doi.org/10.3346/jkms.2015.30.1.66>
  34. Levy A, Faivre-Finn C, Hasan B, De Maio E, Berghoff AS, Girard N, et al. Diversity of brain metastases screening and management in non-small cell lung cancer in Europe: results of the European organisation for research and treatment of cancer lung cancer group survey. *Eur J Cancer* 2018; **93**: 37–46. doi: <https://doi.org/10.1016/j.ejca.2018.01.067>
  35. Hochstenbag MM, Twijnstra A, Wilmink JT, Wouters EF, ten Velde GP. Asymptomatic brain metastases (BM) in small cell lung cancer (SCLC): MR-imaging is useful at initial diagnosis. *J Neurooncol* 2000; **48**: 243–8. doi: <https://doi.org/10.1023/A:1006427407281>
  36. Cagney DN, Martin AM, Catalano PJ, Brown PD, Alexander BM, Lin NU, et al. Implications of screening for brain metastases in patients with breast cancer and non-small cell lung cancer. *JAMA Oncol* 2018; **4**: 1001–3. doi: <https://doi.org/10.1001/jamaoncol.2018.0813>
  37. Neugut AI, Sackstein P, Hillyer GC, Jacobson JS, Bruce J, Lassman AB, et al. Magnetic resonance imaging-based screening for asymptomatic brain tumors: a review. *Oncologist* 2019; **24**: 375–84. doi: <https://doi.org/10.1634/theoncologist.2018-0177>
  38. Pope WB. Brain metastases: neuroimaging. *Handb Clin Neurol* 2018; **149**: 89–112. doi: <https://doi.org/10.1016/B978-0-12-811161-1.00007-4>
  39. Fink JR, Muzi M, Peck M, Krohn KA. Multimodality brain tumor imaging: MR imaging, PET, and PET/MR imaging. *J Nucl Med* 2015; **56**: 1554–61. doi: <https://doi.org/10.2967/jnumed.113.131516>
  40. Brindle KM, Izquierdo-García JL, Lewis DY, Mair RJ, Wright AJ. Brain tumor imaging. *J Clin Oncol* 2017; **35**: 2432–8. doi: <https://doi.org/10.1200/JCO.2017.72.7636>

41. GCTE G, Bockel S, Majer M, Ammari S, Smits M. Imaging of brain metastases: diagnosis and monitoring. *Central Nervous System Metastases* 2019; 145–58. doi: [https://doi.org/10.1007/978-3-030-23417-1\\_12](https://doi.org/10.1007/978-3-030-23417-1_12)
42. Mills SJ, Thompson G, Jackson A. Advanced magnetic resonance imaging biomarkers of cerebral metastases. *Cancer Imaging* 2012; 12: 245–52. doi: <https://doi.org/10.1102/1470-7330.2012.0012>
43. Planchard D, Popat S, Kerr K, Novello S, Smit EF, Faivre-Finn C, et al. Metastatic non-small cell lung cancer: ESMO clinical practice guidelines for diagnosis, treatment and follow-up. *Annals of Oncology* 2018; 29(Suppl 4): iv192–237. doi: <https://doi.org/10.1093/annonc/mdy275>
44. Frankel TL, Bamboat ZM, Ariyan C, Coit D, Sabel MS, Brady MS. Predicting the development of brain metastases in patients with local/regional melanoma. *J Surg Oncol* 2014; 109: 770–4.
45. Breckwoldt M, Bendszus M. [Cerebral MR imaging of malignant melanoma] Zerebrale MR-Bildgebung beim malignen Melanom. *Radiologe* 2015; 55: 113–9.
46. Kato MK, Tanase Y, Uno M, Ishikawa M, Kato T. Brain metastases from uterine cervical and endometrial cancer. *Cancers* 2021; 13: 519. doi: <https://doi.org/10.3390/cancers13030519>
47. Straub S, Laun FB, Freitag MT, Kölsche C, von Deimling A, Denoix M, et al. Assessment of melanin content and its influence on susceptibility contrast in melanoma metastases. *Clin Neuroradiol* 2020; 30: 607–14. doi: <https://doi.org/10.1007/s00062-019-00816-x>
48. Haller S, Zaharchuk G, Thomas DL, Lovblad K-O, Barkhof F, Golay X. Arterial spin labeling perfusion of the brain: emerging clinical applications. *Radiology* 2016; 281: 337–56. doi: <https://doi.org/10.1148/radiol.2016150789>
49. McKnight CD, Motuzas CL, Srinivasan A. Approach to brain neoplasms: what the oncologist wants to know. *Semin Roentgenol* 2018; 53: 6–22. doi: <https://doi.org/10.1053/j.ro.2017.11.002>
50. Huang BY, Kwock L, Castillo M, Smith JK. Association of choline levels and tumor perfusion in brain metastases assessed with proton MR spectroscopy and dynamic susceptibility contrast-enhanced perfusion weighted MRI. *Technol Cancer Res Treat* 2010; 9: 327–37. doi: <https://doi.org/10.1177/153303461000900403>
51. Li Y, Park I, Nelson SJ. Imaging tumor metabolism using in vivo magnetic resonance spectroscopy. *Cancer J* 2015; 21: 123–8. doi: <https://doi.org/10.1097/PPO.0000000000000097>
52. Jones KM, Pollard AC, Pagel MD. Clinical applications of chemical exchange saturation transfer (CEST) MRI. *J Magn Reson Imaging* 2018; 47: 11–27. doi: <https://doi.org/10.1002/jmri.25838>
53. Chen H, Pang Y, Wu J, Zhao L, Hao B, Wu J, et al. Comparison of [<sup>68</sup>Ga]Ga-DOTA-FAPI-04 and [<sup>18</sup>F] FDG PET/CT for the diagnosis of primary and metastatic lesions in patients with various types of cancer. *Eur J Nucl Med Mol Imaging* 2020; 47: 1820–32. doi: <https://doi.org/10.1007/s00259-020-04769-z>
54. Pyatigorskaya N, Habert M-O, Rozenblum L. Contribution of PET-MRI in brain diseases in clinical practice. *Curr Opin Neurol* 2020; 33: 430–8. doi: <https://doi.org/10.1097/WCO.0000000000000841>
55. Wang JL, Elder JB. Techniques for open surgical resection of brain metastases. *Neurosurg Clin N Am* 2020; 31: 527–36. doi: <https://doi.org/10.1016/j.nec.2020.06.003>
56. Soffietti R, Abacioglu U, Baumert B, Combs SE, Kinhult S, Kros JM, et al. Diagnosis and treatment of brain metastases from solid tumors: guidelines from the European Association of Neuro-Oncology (EANO). *Neuro Oncol* 2017; 19: 162–74. doi: <https://doi.org/10.1093/neuonc/now241>
57. Kiesel B, Thomé CM, Weiss T, Jakola AS, Darlix A, Pellerino A, et al. Perioperative imaging in patients treated with resection of brain metastases: a survey by the European Association of Neuro-Oncology (EANO) Youngsters Committee. *BMC Cancer* 2020; 20: 410. doi: <https://doi.org/10.1186/s12885-020-06897-z>
58. Salem U, Kumar VA, Madewell JE, Schomer DE, de Almeida Bastos DC, Zinn PO, et al. Neurosurgical applications of MRI guided laser interstitial thermal therapy (LITT). *Cancer Imaging* 2019; 19: 65. doi: <https://doi.org/10.1186/s40644-019-0250-4>
59. Teyateeti A, Brown PD, Mahajan A, Laack NN, Pollock BE. Brain metastases resection cavity radio-surgery based on T2-weighted MRI: technique assessment. *J Neurooncol* 2020; 148: 89–95. doi: <https://doi.org/10.1007/s11060-020-03492-x>
60. Putz F, Mengling V, Perrin R, Masitho S, Weissmann T, Rösch J. Magnetic resonance imaging for brain stereotactic radiotherapy: A review of requirements and pitfalls Magnetresonanztomographie für die stereotaktische Strahlentherapie des Gehirns: Anforderungen und Fehlerquellen – eine Übersicht. *Strahlenther Onkol* 2020; 196: 444–56.
61. Benveniste RJ, Yechieli R, Diwanji T. Early magnetic resonance imaging after gamma knife radiosurgery of brain metastases. *World Neurosurg* 2021; 146: e1177–81. doi: <https://doi.org/10.1016/j.wneu.2020.11.119>
62. Long GV, Trefzer U, Davies MA, Kefford RF, Ascierto PA, Chapman PB, et al. Dabrafenib in patients with Val600Glu or Val600Lys BRAF-mutant melanoma metastatic to the brain (BREAK-MB): a multicentre, open-label, phase 2 trial. *Lancet Oncol* 2012; 13: 1087–95. doi: [https://doi.org/10.1016/S1470-2045\(12\)70431-X](https://doi.org/10.1016/S1470-2045(12)70431-X)
63. Okada H, Weller M, Huang R, Finocchiaro G, Gilbert MR, Wick W, et al. Immunotherapy response assessment in neuro-oncology: a report of the RANO working group. *Lancet Oncol* 2015; 16: e534–42. doi: [https://doi.org/10.1016/S1470-2045\(15\)00088-1](https://doi.org/10.1016/S1470-2045(15)00088-1)
64. Lin NU, Lee EQ, Aoyama H, Barani JJ, Barboriak DP, Baumert BG, et al. Response assessment criteria for brain metastases: proposal from the RANO group. *Lancet Oncol* 2015; 16: e270–8. doi: [https://doi.org/10.1016/S1470-2045\(15\)70057-4](https://doi.org/10.1016/S1470-2045(15)70057-4)
65. Lee DH, Park JE, Kim N, Park SY, Kim Y-H, Cho YH, et al. Tumor habitat analysis by magnetic resonance imaging distinguishes tumor progression from radiation necrosis in brain metastases after stereotactic radiosurgery. *Eur Radiol* 2021. doi: <https://doi.org/10.1007/s00330-021-08204-1>
66. Chukwueke UN, Wen PY. Use of the Response Assessment in Neuro-Oncology (RANO) criteria in clinical trials and clinical practice. *CNS Oncol* 2019; 8: CNS28. doi: <https://doi.org/10.2217/cns-2018-0007>
67. Kohutek ZA, Yamada Y, Chan TA, Brennan CW, Tabar V, Gutin PH, et al. Long-term risk of radionecrosis and imaging changes after stereotactic radiosurgery for brain metastases. *J Neurooncol* 2015; 125: 149–56. doi: <https://doi.org/10.1007/s11060-015-1881-3>
68. Muto M, Frauenfelder G, Senese R, Zeccolini F, Schena E, Giurazza F, et al. Dynamic susceptibility contrast (DSC) perfusion MRI in differential diagnosis between radionecrosis and neoangiogenesis in cerebral metastases using rCBV, rCBF and K2. *Radiol Med* 2018; 123: 545–52. doi: <https://doi.org/10.1007/s11547-018-0866-7>
69. Hu LS, Baxter LC, Smith KA, Feuerstein BG, Karis JP, Eschbacher JM, et al. Relative cerebral blood volume values to differentiate high-grade glioma recurrence from posttreatment radiation effect: direct correlation between image-guided tissue histopathology and localized dynamic susceptibility-weighted contrast-enhanced

- perfusion MR imaging measurements. *AJNR Am J Neuroradiol* 2009; **30**: 552–8. doi: <https://doi.org/10.3174/ajnr.A1377>
70. Morabito R, Alafaci C, Pergolizzi S, Pontoriero A, Iati' G, Bonanno L, et al. DCE and DSC perfusion MRI diagnostic accuracy in the follow-up of primary and metastatic intra-axial brain tumors treated by radiosurgery with cyberknife. *Radiat Oncol* 2019; **14**: 65. doi: <https://doi.org/10.1186/s13014-019-1271-7>
  71. Knitter JR, Erly WK, Stea BD, Lemole GM, Germano IM, Doshi AH, et al. Interval change in diffusion and perfusion MRI parameters for the assessment of pseudoprogression in cerebral metastases treated with stereotactic radiation. *AJR Am J Roentgenol* 2018; **211**: 168–75. doi: <https://doi.org/10.2214/AJR.17.18890>
  72. Taunk NK, Oh JH, Shukla-Dave A, Beal K, Vachha B, Holodny A, et al. Early posttreatment assessment of MRI perfusion biomarkers can predict long-term response of lung cancer brain metastases to stereotactic radiosurgery. *Neuro Oncol* 2018; **20**: 567–75. doi: <https://doi.org/10.1093/neuonc/nox159>
  73. Shah AD, Shridhar Konar A, Paudyal R, Oh JH, LoCastro E, Nuñez DA, et al. Diffusion and perfusion MRI predicts response preceding and shortly after radiosurgery to brain metastases: a pilot study. *J Neuroimaging* 2021; **31**: 317–23. doi: <https://doi.org/10.1111/jon.12828>
  74. Weybright P, Sundgren PC, Maly P, Hassan DG, Nan B, Rohrer S, et al. Differentiation between brain tumor recurrence and radiation injury using MR spectroscopy. *AJR Am J Roentgenol* 2005; **185**: 1471–6. doi: <https://doi.org/10.2214/AJR.04.0933>
  75. Ceccon G, Lohmann P, Stoffels G, Judov N, Filss CP, Rapp M, et al. Dynamic O-(2-18F-fluoroethyl)-L-tyrosine positron emission tomography differentiates brain metastasis recurrence from radiation injury after radiotherapy. *Neuro Oncol* 2017; **19**: 281–8. doi: <https://doi.org/10.1093/neuonc/now149>
  76. Cicone F, Minniti G, Romano A, Papa A, Scaringi C, Tavanti F, et al. Accuracy of F-DOPA PET and perfusion-MRI for differentiating radionecrotic from progressive brain metastases after radiosurgery. *Eur J Nucl Med Mol Imaging* 2015; **42**: 103–11. doi: <https://doi.org/10.1007/s00259-014-2886-4>
  77. Aneja S, Omuro A. Imaging biomarkers for brain metastases: more than meets the eye. *Neuro Oncol* 2019; **21**: 1493–4. doi: <https://doi.org/10.1093/neuonc/noz193>
  78. Peng L, Parekh V, Huang P, Lin DD, Sheikh K, Baker B, et al. Distinguishing true progression from radionecrosis after stereotactic radiation therapy for brain metastases with machine learning and radiomics. *Int J Radiat Oncol Biol Phys* 2018; **102**: 1236–43. doi: <https://doi.org/10.1016/j.ijrobp.2018.05.041>
  79. Lohmann P, Kocher M, Ruge MI, Visser-Vandewalle V, Shah NJ, Fink GR, et al. PET/MRI Radiomics in patients with brain metastases. *Front Neurol* 2020; **11**: 1. doi: <https://doi.org/10.3389/fneur.2020.00001>
  80. Kniep HC, Madesta F, Schneider T, Hanning U, Schönfeld MH, Schön G, et al. Radiomics of brain MRI: utility in prediction of metastatic tumor type. *Radiology* 2019; **290**: 479–87. doi: <https://doi.org/10.1148/radiol.2018180946>
  81. Park YW, An C, Lee J, Han K, Choi D, Ahn SS, et al. Diffusion tensor and postcontrast T1-weighted imaging radiomics to differentiate the epidermal growth factor receptor mutation status of brain metastases from non-small cell lung cancer. *Neuroradiology* 2021; **63**: 343–52. doi: <https://doi.org/10.1007/s00234-020-02529-2>
  82. Karami E, Soliman H, Ruschin M, Sahgal A, Myrehaug S, Tseng C-L, et al. Quantitative MRI biomarkers of stereotactic radiotherapy outcome in brain metastasis. *Sci Rep* 2019; **9**: 19830. doi: <https://doi.org/10.1038/s41598-019-56185-5>
  83. Cha YJ, Jang WI, Kim M-S, Yoo HJ, Paik EK, Jeong HK, et al. Prediction of response to stereotactic radiosurgery for brain metastases using Convolutional neural networks. *Anticancer Res* 2018; **38**: 5437–45. doi: <https://doi.org/10.21873/anticancer.12875>
  84. Galldiks N, Abdulla DSY, Scheffler M, Wolpert F, Werner J-M, Hüllner M, et al. Treatment Monitoring of Immunotherapy and Targeted Therapy Using <sup>18</sup>F-FET PET in Patients with Melanoma and Lung Cancer Brain Metastases: Initial Experiences. *J Nucl Med* 2021; **62**: 464–70. doi: <https://doi.org/10.2967/jnumed.120.248278>
  85. Sperduto PW, Kased N, Roberge D, Xu Z, Shanley R, Luo X, et al. Summary report on the graded prognostic assessment: an accurate and facile diagnosis-specific tool to estimate survival for patients with brain metastases. *J Clin Oncol* 2012; **30**: 419–25. doi: <https://doi.org/10.1200/JCO.2011.38.0527>
  86. Zakaria R, Chen YJ, Hughes DM, Wang S, Chawla S, Poptani H, et al. Does the application of diffusion weighted imaging improve the prediction of survival in patients with resected brain metastases? A retrospective multicenter study. *Cancer Imaging* 2020; **20**: 16. doi: <https://doi.org/10.1186/s40644-020-0295-4>
  87. Vu C, Chai Y, Coloigner J, Nederveen AJ, Borzage M, Bush A, et al. Quantitative perfusion mapping with induced transient hypoxia using BOLD MRI. *Magn Reson Med* 2021; **85**: 168–81. doi: <https://doi.org/10.1002/mrm.28422>
  88. Moek KL, Giesen D, Kok IC, de Groot DJA, Jalving M, Fehrmann RSN, et al. Theranostics using antibodies and Antibody-Related therapeutics. *J Nucl Med* 2017; **58**(Supplement 2): 83S–90. doi: <https://doi.org/10.2967/jnumed.116.186940>
  89. Pruis IJ, van Dongen GAMS, Veldhuijzen van Zanten SEM. The added value of diagnostic and theranostic PET imaging for the treatment of CNS tumors. *Int J Mol Sci* 2020; **21**: 1029. doi: <https://doi.org/10.3390/ijms21031029>
  90. Ulaner GA, Lyashchenko SK, Riedl C, Ruan S, Zanzonico PB, Lake D, et al. First-in-human human epidermal growth factor receptor 2-targeted imaging using <sup>89</sup>Zr-pertuzumab PET/CT: dosimetry and clinical application in patients with breast cancer. *J Nucl Med* 2018; **59**: 900–6. doi: <https://doi.org/10.2967/jnumed.117.202010>
  91. Curley CT, Stevens AD, Mathew AS, Stasiak K, Garrison WJ, Miller GW, et al. Immunomodulation of intracranial melanoma in response to blood-tumor barrier opening with focused ultrasound. *Theranostics* 2020; **10**: 8821–33. doi: <https://doi.org/10.7150/thno.47983>